



Coupled Bloch-phonon oscillations in GaAs/AlGaAs superlattices: theory and experiment

T. Dekorsy^{a, *}, A. Bartels^a, H. Kurz^a, A.W. Ghosh^b, L. Jönsson^b, J.W. Wilkins^b, K. Köhler^c, R. Hey^d, K. Ploog^d

^a*Institut für Halbleitertechnik II, RWTH Aachen, Sommerfeldstr. 24, D-52056 Aachen, Germany*

^b*Department of Physics, Ohio State University, 174 West 18th Avenue, Columbus, OH 43210, USA*

^c*Fraunhofer-Institut für Angewandte Festkörperphysik, D-79108 Freiburg, Germany*

^d*Paul Drude Institut für Festkörperphysik, D-10117 Berlin, Germany*

Abstract

We report on the femtosecond dynamics of coherent Bloch oscillations in GaAs/Al_xGa_{1-x}As superlattices. In a superlattice with a miniband width equal to the optical phonon energy of GaAs the Bloch frequency can be tuned into resonance with the LO phonon by an applied electric field. We observe a strong coupling between Bloch oscillations and phonons leading to the coherent excitation of optical phonons when both are brought into resonance. This phenomenon is analyzed theoretically on the base of a microscopic Hamiltonian for the electron–phonon interaction in the superlattice. We show that coupled modes are described by a nonlinear pendulum coupled linearly to an oscillator representing the phonons. Under resonance condition the amplitudes of both modes increase and sidebands appear. The theoretical results are compared to the experimental observations. © 2000 Elsevier Science B.V. All rights reserved.

Keywords: Bloch oscillations; Electron–phonon coupling; Superlattices; THz dynamics

1. Introduction

Bloch oscillations of electrons in superlattices have been convincingly demonstrated in femtosecond time-resolved experiments like four wave mixing [1,2], THz emission [3], and transmissive electro-optic sampling (TEOS) [4]. TEOS experiments monitor the

change in transmission of a time-delayed circularly polarized probe pulse through a biased superlattice after photoexcitation with a linearly polarized pump pulse. The transmission change is affected directly by longitudinal field oscillations in the superlattice that occur at THz frequencies. This involves Bloch oscillations, plasmons, longitudinal optical phonons, all of which exist in the THz regime. In particular, the first two modes are tunable and can be brought into resonance via the change of an external applied electric field and the change of carrier density,

* Corresponding author. Tel.: +49-241-80806; fax: +49-241-8888246.

E-mail address: dekorsy@iht-ii.rwth-aachen.de (T. Dekorsy)

respectively. The coupling between the modes is expected to result in a modification of the mode amplitudes and broadenings of the spectral response.

In this paper, we describe recent experimental and theoretical progress made towards the understanding of these interactions. Besides the fundamental physical interest, such mode-coupling is crucial to understand for designing THz devices operating on Bloch oscillators. Our results can be summarized as follows: starting with a microscopic Hamiltonian describing electrons and phonons interacting with each other in a superlattice under an external DC field, we establish that the Bloch oscillating electrons behave like a nonlinear pendulum coupled linearly to an oscillator representing the phonons. We solve the equations perturbatively in the limit of low density and establish that contrary to conventional expectations with mode-coupling the coupled Bloch-phonon modes do not have a gap in their frequency spectra at resonance as the external field is varied. Instead, the coupling manifests itself through a resonant enhancement of the amplitudes of both the Bloch oscillation and the phonon modes. In addition, sidebands of varying heights and widths are generated near resonance due to parametric Bloch-phonon coupling. The theoretical results are compared to experiments performed in a GaAs/Al_xGa_{1-x}As superlattice with a first electronic miniband width equal to the LO phonon energy of GaAs. This miniband width allows us to tune the Bloch frequency into resonance with the LO phonon.

2. Theoretical description of Bloch-phonon equations

We consider a system of collision-free superlattice electrons with a tight-binding kinetic energy $\varepsilon_k = -(A/2)\cos kd$, interacting through a Coulomb repulsion $V_q = 4\pi e^2/q^2$ and coupled to an external DC field E_0 along the growth direction of the superlattice through a dipole matrix $\mu_{kk'} = (ie/\hbar)\delta_{kk'}\partial/\partial k$. The scalar notation k refers here to the momentum component along the growth direction of the superlattice. We also introduce a set of dispersionless LO phonons of frequency ω_{LO} , stretched by an external DC field through a phonon dipole moment μ_q per unit cell, and coupled to electrons through a Fröhlich polar coupling $M_q = -i\sqrt{4\pi e^2\hbar\omega_{LO}/2\varepsilon_P q^2}$, with $1/\varepsilon_P \equiv$

$1/\varepsilon_\infty - 1/\varepsilon_0$, the subscripts ∞ and 0 corresponding, respectively, to high- and low-frequency dielectric constants of the superlattice. The Hamiltonian then is

$$\begin{aligned} \mathcal{H} = & \sum_k \varepsilon_k c_k^\dagger c_k + \frac{1}{2} \sum_{qkk'} V_q c_{k+q}^\dagger c_{k'-q}^\dagger c_k c_{k'} \\ & - E_0 \sum_{kk'} \mu_{kk'} c_k^\dagger c_{k'} + \sum_q \hbar\omega_{LO} b_q^\dagger b_q \\ & - E_0 \sum_q \mu_q (b_q + b_q^\dagger) + \sum_{kq} M_q c_k^\dagger c_{k+q} (b_q + b_{-q}^\dagger). \end{aligned} \quad (1)$$

We use the Hamiltonian to write down the equations for the electron density matrix $N_{KQ} \equiv \langle c_{K+Q/2}^\dagger c_{K-Q/2} \rangle$. We factorize all four-operator expectation values into products of two-operator expectation values using the random phase approximation, which allows us to describe the dynamics in terms of the mean-field polarization $P = \mu n = (ie/\hbar) \sum_K \partial N_{KQ} / \partial Q|_{Q=0}$. Note that we are employing for convenience the ‘center-of-mass’ and ‘relative’ coordinates $K = (k + k')/2$ and $q = k - k'$. We also ignore electron–phonon correlations, which allows us to factorize terms like $\langle c^\dagger c b \rangle \approx \langle c^\dagger c \rangle \langle b \rangle$. The equation for the distribution function $f_K = N_{K0}$ then is

$$\begin{aligned} \left[\frac{\partial}{\partial t} + \frac{eE(t)}{\hbar} \frac{\partial}{\partial K} \right] N_{K0} = & -\frac{i}{\hbar} \sum_q M_q (B_q + B_{-q}^*) \\ & \times [N_{K-q/2,q} - N_{K+q/2,q}], \quad (2) \end{aligned}$$

where $B_q = \langle b_q \rangle$ and B_q^* are the amplitudes of the *coherent* phonons, and $E(t) = E_0 - 4\pi P(t)$. In the long-wavelength limit $q \rightarrow 0$, expanding the terms in the square bracket about $q = 0$ leads to a cancellation of the divergence in $M_q \propto 1/q$, leading to a modified pendulum equation for the net vector potential $\eta(t) = ed/\hbar \int_0^t dt' E(t')$. Since the stretching $w \propto B_0 + B_0^*$ of the polar ions also contributes to the net electric field: $\dot{\eta} = (ed/\hbar)(E_0 - 4\pi n\mu) - Cw$, with $C = \sqrt{\omega_{LO}^2 - \omega_{TO}^2}$ non-zero because the transverse phonons oscillate at the bare frequency ω_{TO} while the longitudinal phonons oscillate at a larger frequency ω_{LO} due to the extra stretching from the polar fields. The transverse and longitudinal phonon frequencies satisfy the Lyddane–Sachs–Teller relation: $\omega_{LO}/\omega_{TO} = \sqrt{\varepsilon_0/\varepsilon_\infty}$ [5]. The result of this

calculation describes a pendulum (electronic mode) linearly coupled to an oscillator (LO phonon mode):

$$\begin{aligned} \dot{\eta} + \omega_{\text{pl}}^2 \sin \eta &= -C\dot{w}, \\ \ddot{w} + \omega_{\text{TO}}^2 w &= C\dot{\eta}, \end{aligned} \quad (3)$$

where ω_{pl} is the plasma frequency. For the boundary conditions we assume an impulsive generation of LO phonons [6,7], and no initial polarization induced by the photoexcitation process itself: $\eta(0) = \dot{w}(0) = 0$, $w(0) = C\omega_{\text{B}}/\omega_{\text{LO}}^2$, and $\dot{\eta}(0) = \tilde{\omega}_{\text{B}} = \omega_{\text{B}}\epsilon_{\infty}/\epsilon_0$, where ω_{B} is the Bloch frequency. The system of equations (3) can then be solved in the low-density limit ($\omega_{\text{pl}} \ll \omega_{\text{B}}$) by a perturbative expansion in the small parameter $\omega_{\text{pl}}/\tilde{\omega}_{\text{B}}$. We expand the variables as follows:

$$\begin{aligned} \eta(t) &= \eta_0(t) + \left(\frac{\omega_{\text{pl}}}{\tilde{\omega}_{\text{B}}}\right)^2 \eta_1(t) + \dots, \\ w(t) &= w_0(t) + \left(\frac{\omega_{\text{pl}}}{\tilde{\omega}_{\text{B}}}\right)^2 w_1(t) + \dots \end{aligned} \quad (4)$$

and solve for $\eta(t)$ and $w(t)$ perturbatively in the small parameter $(\omega_{\text{pl}}/\tilde{\omega}_{\text{B}})^2$. The result of the calculation is as follows:

$$\begin{aligned} \eta_0(t) &= \tilde{\omega}_{\text{B}}t, \\ w_0(t) &= \frac{C\omega_{\text{B}}}{\omega_{\text{LO}}^2}, \\ \eta_1(t) &= \tilde{\omega}_{\text{B}} \left(\frac{\omega_{\text{TO}}^2 - \tilde{\omega}_{\text{B}}^2}{\omega_{\text{LO}}^2 - \tilde{\omega}_{\text{B}}^2} \right) \left[\frac{\sin(\tilde{\omega}_{\text{B}}t)}{\tilde{\omega}_{\text{B}}} - t \right] \\ &\quad + \frac{C^2\tilde{\omega}_{\text{B}}^3}{\omega_{\text{LO}}^2(\omega_{\text{LO}}^2 - \tilde{\omega}_{\text{B}}^2)} \left[\frac{\sin(\omega_{\text{LO}}t)}{\omega_{\text{LO}}} - t \right], \\ w_1(t) &= \frac{C\tilde{\omega}_{\text{B}}}{\omega_{\text{LO}}^2 - \tilde{\omega}_{\text{B}}^2} [\cos(\tilde{\omega}_{\text{B}}t) - 1] \\ &\quad - \frac{C\tilde{\omega}_{\text{B}}^3}{\omega_{\text{LO}}^2(\omega_{\text{LO}}^2 - \tilde{\omega}_{\text{B}}^2)} [\cos(\omega_{\text{LO}}t) - 1]. \end{aligned} \quad (5)$$

The zeroth-order corrections in the plasma frequency show that in the absence of screening charges ($\omega_{\text{pl}} = 0$), there are no oscillations in the system, just

a stretch of the ions within each unit cell, proportional to the external field. Dynamics is introduced once electrons are photoexcited into the conduction miniband, i.e., through the terms η_1 and w_1 . This leads to Bloch oscillations in η_1 while w_1 exhibits signatures of LO phonons. The LO phonons are excited coherently, because the ionic displacement w is proportional to $\langle b_0^\dagger + b_0 \rangle$, which is non-zero [8]. Prior to the excitation, the stretch of the ions is given by $w_0 = C\omega_{\text{B}}/\omega_{\text{LO}}^2$. Ultrafast screening by the photoexcited charges leads to a new reduced equilibrium value of magnitude $C\omega_{\text{B}}/\omega_{\text{LO}}^2[1 - \omega_{\text{pl}}^2/\omega_{\text{B}}\tilde{\omega}_{\text{B}}]$, obtained from the DC component of w . It is this impulsive change in equilibrium stretching that excites the phonons coherently at frequency ω_{LO} .

Although the perturbation theory breaks down at resonance $\tilde{\omega}_{\text{B}} \approx \omega_{\text{LO}}$ as can be seen clearly from the divergences in η and w , we can get an idea about the field dependencies of these quantities away from resonance. For the Bloch oscillations, we look at the part of $\dot{\eta}$ that oscillates at ω_{B} , which yields the corresponding Fourier amplitude. The coefficient of the $\cos \tilde{\omega}_{\text{B}}t$ term in $\dot{\eta}(t)$ is given by $(\omega_{\text{pl}}^2/\tilde{\omega}_{\text{B}})([\omega_{\text{TO}}^2 - \tilde{\omega}_{\text{B}}^2]/[\omega_{\text{LO}}^2 - \tilde{\omega}_{\text{B}}^2])$. The second factor in the round brackets is the resonance factor, which leads to a peak at resonance ($\tilde{\omega}_{\text{B}} \approx \omega_{\text{LO}}$). The prefactor $\omega_{\text{pl}}^2/\tilde{\omega}_{\text{B}}$ gives the familiar result that the Bloch oscillation amplitude varies as Δ/E_0 for a superlattice with miniband width Δ and external field E_0 . Thus, the Bloch amplitude has a peak superimposed on a decreasing structure when plotted versus the bias voltage. For the phonon mode, as obtained from the ω_{LO} component of $w(t)$, the amplitude varies as $\sim \omega_{\text{B}}$ for small fields and $\sim 1/\omega_{\text{B}}$ for large fields, leading to a relatively weak dependence on field, except a strong enhancement at resonance. Evidently, the amplitudes diverge at resonance, indicating that a more careful numerical analysis, taking into account the specific details of the measurement process and collisions, is needed to get agreement with experiments.

For small plasmon frequencies, the perturbation theory does not allow for any change in the resonance frequencies due to coupling. The oscillations are at frequencies ω_{LO} and $\tilde{\omega}_{\text{B}}$. There is no mode at the TO frequency. This is expected, since Fröhlich polar phonons couple only with longitudinal modes. The transverse mode that arises in plasmon–phonon dispersions, for example, are basically longitudinal

phonons oscillating at the bare TO frequency due to electronic screening. For a fixed plasma frequency, however, varying the Bloch frequency parametrically does not alter the screening, hence we do not expect the TO modes to emerge. The Bloch frequency enters only through the initial conditions in Eq. (3), and not directly in the equations themselves, which explains why merely varying the Bloch frequency does not open up a gap in the frequency spectrum plotted versus ω_B . Bloch oscillations thus couple with phonons in a way that is qualitatively different from plasmon–phonon modes [9]. Bloch oscillations arise simply because the sample is periodic, while the LO and plasma oscillations arise due to actual restoring forces associated with oscillator-like motions. The coupling manifests itself through a non-monotonic field dependence of the individual peak amplitudes plotted for varying fields.

The coupling of Bloch oscillations and phonons also occurs through the appearance of Bloch-phonon sidebands due to the parametric coupling between the two modes through the sine term in the equations of motion, which tends to mix modes. For example, let us substitute $\eta(t) \approx \tilde{\omega}_B t + \alpha_0 \tilde{\omega}_B \sin(\tilde{\omega}_B t) + \beta_0 \sin(\omega_{LO} t)$ in the equation for η in Eq. (3), where α_0 and β_0 are obtained from our perturbative solution for η . This gives

$$\begin{aligned}
 -Cw &= \alpha_0 \tilde{\omega}_B \cos(\tilde{\omega}_B t) + \beta_0 \omega_{LO} \cos(\omega_{LO} t) \\
 &- \omega_{pl}^2 \sum_{m=-\infty}^{\infty} \sum_{p=-\infty}^{\infty} \left[\frac{J_{m-1}(\alpha_0) J_p(\beta_0)}{m\tilde{\omega}_B + p\omega_{LO}} \right] \\
 &\times \cos(m\tilde{\omega}_B + p\omega_{LO})t. \quad (6)
 \end{aligned}$$

As one can see from the last term, the response has sidebands at positions $m\tilde{\omega}_B + n\omega_{LO}$ for integer m and n , arising out of the Bloch-phonon couplings. An investigation of the arguments of the Bessel terms reveals that the sidebands are prominent near resonance, at plasma frequencies larger than the collision rate but small enough to not screen out the Bloch oscillations. The sidebands demonstrate that Bloch oscillations couple with phonons even in the absence of a gap in the spectrum. Collisions, however, will tend to wash away the sidebands. Fig. 1 shows Bloch-phonon sidebands for $\nu_{pl} = 2$ THz, obtained by a numerical solution of the Bloch-phonon coupled equations of motion in the absence of collisions.

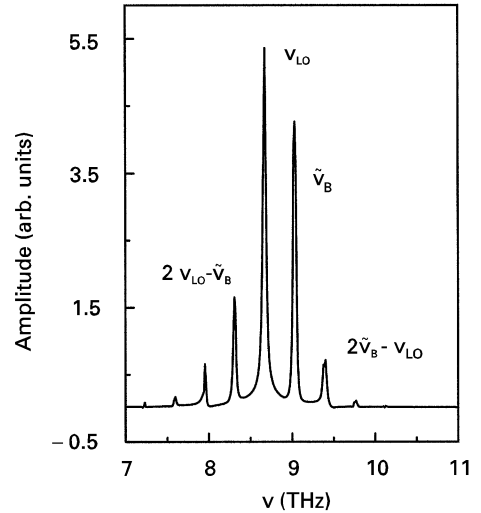


Fig. 1. Bloch-phonon sidebands arising out of parametric coupling between LO phonons and Bloch oscillations in absence of collisions for a plasma frequency $\nu_{pl} = 2$ THz and a Bloch frequency $\nu_B = 11.4$ THz.

3. Experimental results

We perform TEOS experiments for the investigation of Bloch-phonon coupling, since it is sensitive to the internal longitudinal polarization along the growth direction of the superlattices [4]. The laser source is a Kerr-lens mode-locked Ti:sapphire laser delivering optical pulses of 50 fs duration corresponding to a spectral width of 40 meV. The broadband laser spectrum is tuned to the first interband transitions in the superlattice, i.e. from the first heavy-hole to the first electron states. The short pulse prepares a coherent superposition of electronic Wannier–Stark states in the biased superlattice [10,11]. The heavy holes are already fully localized at the electric fields under consideration. A coherent electronic wavepacket is created which performs spatial oscillations along the superlattice growth direction with the Bloch frequency [12]. The investigated sample consists of 35 periods GaAs wells of 6.7 nm width and $\text{Al}_{0.3}\text{Ga}_{0.7}\text{As}$ barriers of 1.7 nm width. The coupling of the lowest quantized electronic levels in the quantum wells forms an electronic miniband of 36 meV width which equals the LO phonon energy in bulk GaAs. For applying a static

electric field, the superlattice is embedded in a Schottky diode. This miniband width allows to tune the Bloch frequency into resonance with the LO phonon. This is not possible for smaller miniband widths since for such superlattices the wave functions are already fully localized so that no oscillating wavepacket with the phonon frequency can be excited. On the other hand, larger miniband widths are inherently associated with stronger dephasing times. Hence, the choice of a minibandwidth equal to the phonon energy is a trade-off concerning the visibility of Bloch-phonon coupling.

Figs. 2(a) and (b) depict the time-domain TEOS data and the corresponding frequency domain responses recorded at an excitation density of $1 \times 10^{10} \text{ cm}^{-2}$ at 10 K. This excitation density corresponds to a plasma frequency much lower than the phonon frequency, so that coupling with plasmons can be neglected in the frequency range close to the optical phonon resonance. The data are shown for different voltages applied to the sample. For the voltages range below -3.8 V , the data are dominated by the rapidly dephasing electronic coherence of the Bloch oscillations with a dephasing time of $(400 \pm 50) \text{ fs}$. The frequency of the oscillations increases with increasing bias voltage according to $v_B = eEd/h$ as expected for Bloch oscillations. At reverse bias voltages larger than -4.0 V , oscillations appear, which can be traced over more than 10 ps in contrast to the subpicosecond dephasing of the Bloch oscillations at lower voltages. The Fourier transforms show at -4.0 V a strong maximum at the LO phonon. At -4.2 V the signal is fully dominated by the long-living oscillation with LO frequency. At this voltage the Bloch frequency is in resonance with the LO phonon. The change from the electronic coherence with a sub-ps dephasing time to the long living phonon oscillations becomes also clearly visible in the frequency domain data (Fig. 2(b)). The pure electronic coherence is associated with the broad spectral peak while the spectral width of the coherent phonon oscillation is determined by the finite time-window of the measurement. Higher reverse bias voltages could not be applied to the sample due to the occurrence of breakdown of the Schottky diode. In addition, we infer from CW elect-absorption measurements that at higher internal electric fields the electronic states become fully localized.

The experimental results clearly demonstrate a coupling of Bloch oscillations to LO phonons under resonance conditions. The observed generation of coherent phonons under resonance conditions confirms the theoretical result of an enhancement of the LO phonon amplitude. The enhancement of the Bloch amplitude under resonance conditions cannot be deduced from the experiments. One reason is the miniband width which equals the LO phonon energy leading to a strong localization of the Wannier–Stark wave functions close to resonance. Another reason is the expected strong dephasing of the Bloch oscillations when the carriers can energetically relax between adjacent Wannier–Stark levels by LO phonon emission [13]. Both of these aspects are not included in the theoretical model so far. The appearance of sidebands also cannot be deduced from the experimental data, which is attributed to the rapid dephasing of the electronic coherence in the experiments. These discrepancies demonstrate the importance to include collision effects in the theory.

4. Conclusions

The theoretical analysis of the polar coupling between Bloch oscillations and LO phonons in a superlattice leads to a resonance and sidebands. The coupling of Bloch oscillations with LO phonons can be described by the linear coupling of a pendulum (electronic mode) with an oscillator (phonon mode). Perturbation theory in the small parameter $(\omega_{pl}/\tilde{\omega}_B)^2$ reveals that near the Bloch-phonon resonance, there is no gap in the spectrum, but the amplitudes of the Bloch and phonon modes diverge. The absence of the gap is due to the fact that the Bloch oscillation is not an elementary excitation that could cause a level repulsion with the phonons, but merely a periodic response of electrons to a periodic array of quantum wells. The resonant enhancement of the individual Fourier amplitudes indicates coupling between Bloch oscillations and LO phonons. However, the perturbation theory breaks down at resonance. Thus, a more detailed analysis will need to incorporate collisions in the equations of motion, followed by numerical modeling. The coupling of Bloch oscillations is confirmed by the experimental results obtained in a superlattice with 36 meV electronic miniband width.

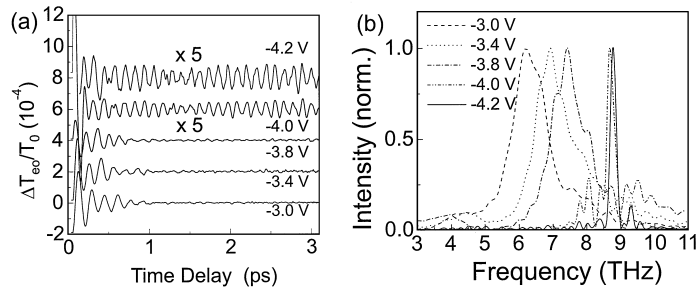


Fig. 2. (a) Coupled Bloch-phonon oscillations at 10 K lattice temperature for an excitation density of $1 \times 10^{10} \text{ cm}^{-2}$ for different voltages applied. The data at -4.0 and -4.2 V are magnified by a factor of 5. (b) Normalized Fourier transforms of the data in (a).

Acknowledgements

This work was supported in part by the German Volkswagen Foundation and the United States National Science Foundation (PHY-9722127). AB thanks the Konrad-Adenauer Stiftung for financial support. AWG thanks the Ohio State University Presidential Fellowship for support.

References

- [1] J. Feldmann, K. Leo, J. Shah, D.A.B. Miller, J.E. Cunningham, S. Schmitt-Rink, T. Meier, G. von Plessen, A. Schulze, P. Thomas, *Phys. Rev. B* 46 (1992) 7252.
- [2] K. Leo, P. Haring Bolivar, F. Brüggemann, R. Schwedler, K. Köhler, *Solid State Commun.* 84 (1992) 943.
- [3] C. Waschke, H.G. Roskos, R. Schwedler, K. Leo, H. Kurz, K. Köhler, *Phys. Rev. Lett.* 70 (1993) 3319.
- [4] T. Dekorsy, P. Leisching, H. Kurz, K. Köhler, *Phys. Rev. B* 50 (1994) 8106.
- [5] M. Born, K. Huang, *Dynamical Theory of Crystal Lattices*, Clarendon Press, Oxford, 1954.
- [6] A.V. Kuznetsov, C.J. Stanton, *Phys. Rev. B* 51 (1995) 7555.
- [7] G.C. Cho, W. Kütt, H. Kurz, *Phys. Rev. Lett.* 65 (1990) 764.
- [8] A.V. Kuznetsov, C.J. Stanton, *Phys. Rev. Lett.* 73 (1994) 3243.
- [9] A. Mooradian, A.L. McWhorter, *Phys. Rev. Lett.* 19 (1967) 849.
- [10] E.E. Mendez, F. Agulló-Rueda, J.M. Hong, *Phys. Rev. Lett.* 60 (1988) 2426.
- [11] P. Voisin, J. Bleuse, C. Bouche, S. Gaillard, C. Alibert, A. Regreny, *Phys. Rev. Lett.* 61 (1988) 1639.
- [12] G. Bastard, R. Fereirra, in: G. Fasol, A. Fasolini (Eds.), *Spectroscopy of Semiconductor Microstructures*, Plenum Press, New York, 1989, p. 333.
- [13] J. Hader, T. Meier, S.W. Koch, F. Rossi, N. Linder, *Phys. Rev. B* 55 (1997) 13799.